Checkpoint kinase 1 is activated and promotes cell survival after exposure to sulphur mustard

Paul A Jowsey[a] and Peter G Blain

Medical Toxicology Centre, Wolfson Unit, Newcastle University, Newcastle upon Tyne, NE2 4AA

[a] To whom correspondence should be addressed

e-mail: **p.a.jowsey@ncl.ac.uk**

Tel: **+44-191-2228537**

Fax: **+44-191-2226442**

Abstract

Sulphur mustard (SM) is a vesicating agent that has been used several times as a weapon during military conflict and continues to pose a threat as an agent of warfare/terrorism. After exposure, SM exerts both acute and delayed long-term toxic effects principally to the skin, eyes and respiratory system. These effects are thought to be mediated, at least in part, by direct interaction of SM with DNA, forming a myriad of DNA lesions and initiating effects on cell cycle and cell death pathways. Previous studies have demonstrated that a complex network of cellular DNA damage response pathways are utilised in cells exposed to SM, consistent with SM causing multiple forms of DNA damage. The present study focused on the role of Checkpoint kinase 1 (CHK1), a protein with putative roles in homologous recombination repair, p53 activation and the initiation of cell cycle checkpoints after certain forms of DNA damage. The data showed that SM caused robust activation of CHK1, monitored by multi-site phosphorylation analysis and that this activation was dependent on the ataxia telangiectasia and Rad3-related (ATR) protein kinase. Furthermore, specific inhibition of CHK1 increased SM toxicity in multiple human cell lines, with concomitant increases in markers of apoptosis, DNA damage and mitosis. Finally, the effect of CHK1 inhibition on SM toxicity was much more marked in cells with non-functional p53.

Introduction

Exposure to sulphur mustard [SM, bis(2-chloroethyl) sulphide)] results in acute toxicity to the skin and mucosal surfaces of the eyes and respiratory system (Balali-Mood and Hefazi, 2006; Saladi et al., 2006), with symptoms ranging from mild irritation to severe inflammation or blistering developing over the course of several hours. After high level exposure, SM can become systemic and exert toxic effects on the hematopoietic system, causing immunosuppression and vulnerability to secondary infections (Balali-Mood and Hefazi, 2005; Ghabili et al., 2011). There is also increasing evidence of delayed long-term health effects after a single exposure to SM and apparent recovery from the initial acute toxicity (Balali-Mood et al., 2005; Mahmoudi et al., 2005). These health effects include skin irritation, chronic obstructive pulmonary disease and an increased incidence of certain cancers, particularly those affecting the respiratory system. The precise mechanisms mediating the acute and long-term toxicity of SM remain to be elucidated and there is currently no treatment option in the event of an exposure.

SM is a bifunctional alkylating agent with mutagenic and carcinogenic properties (Ashby et al., 1991). The reaction of SM with DNA is initiated by the formation of a highly reactive sulphonium ion. This intermediate ion forms readily under aqueous conditions, hence the particular vulnerability of moist tissues (e.g. eye and respiratory tract) to SM toxicity. The most abundant DNA lesion after SM exposure is the monoadduct N7-hydroxyethyl thioethyl guanine (N7-HETE-G), constituting around 60% of total DNA adducts (Fidder et al., 1994), although other monoadducts are also formed. These adducts are prone to depurination, resulting in the formation of abasic sites. DNA crosslinks (both inter and intrastrand) caused by SM constitute only 16% of total DNA lesions but are responsible for the high toxicity of this agent. This is clearly demonstrated by an approximate 100-fold increase in the toxicity of bifunctioinal SM compared to a monofunctional analogue (Jowsey et al., 2012).

Cells respond to genotoxic damage by initiating DNA damage signalling cascades, orchestrated by the ataxia telangiectasia mutated (ATM) and ATR protein kinases. These kinases respond to different forms of DNA damage, for example ATM is normally activated in the presence of DNA double strand breaks (DSBs), whereas ATR is activated by single strand stretches of DNA, formed during the processing of various forms of DNA damage, including DNA adducts and crosslinks (Abraham, 2004; Hurley and Bunz, 2007). Once activated, these kinases phosphorylate a wide range of target proteins, including the checkpoint kinases CHK1 and CHK2, the tumour suppressor p53 and the histone variant

H2AX. Given that SM is able to form a variety of DNA lesions, the pathways and proteins involved in the cellular response are likely to be diverse and complex. Previous studies have demonstrated the activation of both ATM and ATR after exposure to SM and monofunctional analogues (Jowsey et al., 2012; Tewari-Singh et al., 2010). The present study focused on the role of CHK1 in response to SM. The activation of CHK1 has been demonstrated after various DNA damaging agents, including ultra-violet radiation, ionising radiation and mono/bifunctional alkylating agents (Patil et al., 2013; Zhang and Hunter, 2014). The mechanism of activation involves ATR-dependent phosphorylation of CHK1 at Ser317 and Ser345 (Zhao and Piwnica-Worms, 2001). It has been proposed that these phosphorylation events relieve the inhibiton normally imposed by the c-terminal regulatory domain of CHK1 on the n-terminal catalytic domain. Mutation of Ser317 or 345 significantly inhibits CHK1 activation, leads to inefficient checkpoint activation and sensitivity to certain genotoxic agents, particularly those that interfere with DNA replication (Capasso et al., 2002; Walker et al., 2009). Subsequent to Ser317/345 phosphorylation, it has been demonstrated that CHK1 undergoes intramolecular autophosphorylation on Ser296 (Clarke and Clarke, 2005; Kasahara et al., 2010). Whilst phosphorylation of this site has a negligible effect on CHK1 activity, it is important in regulating mitotic entry after UV-induced DNA damage, via association with the Cdc25A phosphatase (Kasahara et al., 2010). In unperturbed cells, CHK1 regulates multiple aspects of cell cycle progression, including DNA replication, mitotic entry and the mitotic spindle checkpoint. After DNA damage, CHK1 regulates cell cycle arrest at the G1/S and G2/M transitions as well as during DNA replication, principally by phosphorylation of the Cdc25 family of phosphatases, resulting in relocalization and/or degradation of Cdc25 (Patil et al., 2013; Zhang and Hunter, 2014). Collectively, the Cdc25 phosphatases act to remove inhibitory phosphate groups and thus activate kinases that drive cell cycle progression. CHK1 has also been implicated in chromatin remodelling, an essential component of efficient DNA repair, as well as the homologous recombination repair pathway (Sorensen et al., 2005).

The present study aimed to investigate CHK1 activation and regulation after exposure to the bifunctional alkylating agent SM as well as whether CHK1 has a protective role in the cellular response to SM. The data showed that SM caused robust activation of CHK1, with ATR-dependent phosphorylation of Ser317 and autophosphorylation of Ser296. Specific inhibition of CHK1 blocked Ser296 autophosphorylation and increased SM toxicity in multiple human cell lines, with concomitant increases in markers of apoptosis, DNA damage

and mitosis. Finally, the effect of CHK1 inhibition on SM toxicity was more marked in cells with non-functional p53.

2. Materials and methods

2.1. Cell lines, chemicals and treatments

Hela, HCT 116, HEK 293, SH-SY5Y and A549 cells were obtained from HPA Cultures (Health Protection Agency, Porton Down, UK) and maintained as exponentially growing cultures in Dulbecco's Modified Eagle Medium supplemented with 10% fetal bovine serum and 2mM L-glutamine (Sigma). The CHK1 inhibitor PF 477736 (Tocris Bioscience) was prepared at a stock concentration of 50mM in DMSO and added to cells at final concentrations ranging from 20-250nM (Blasina et al., 2008). The ATR inhibitor AZ 20 (Tocris Bioscience) was prepared at a stock concentration of 50mM in DMSO and added to cells at a final concentration of 4μM (Foote et al., 2013). Inhibitors were added to cells 45min prior to treatment with DNA damaging agents and the DMSO concentration was maintained at 0.1% (v/v) in all samples, with no effect on cell viability. SM was obtained from The Defence Science and Technology Laboratories (Dstl, Porton Down, UK) and stored at 4°C. On the day of use, appropriate dilutions were prepared in isopropanol and added to culture medium such that the final isopropanol concentration was 0.2% (v/v) in all samples. This concentration had no effect on cell viability. SM treatments were performed in normal growth medium containing serum. This was to ensure that cells retained their proliferative capacity during the course of the study. This is important for mechanistic studies on the cellular response to SM as cell proliferation, and DNA replication in particular, are highly relevant to the toxic mechanism of SM.

2.2. Cell viability assay

Cells were seeded in 24-well plates and allowed to adhere overnight. After treatment with 100nM PF 477736 for 45 min, cells in normal growth medium (see 2.1) were treated with the indicated concentrations of SM (or isopropanol control for 'untreated' cells) for 24-48h prior to the measurement of cell viability using an MTS-based assay (Promega). Briefly, culture medium was removed and replaced with 300μl of medium containing 20% (v/v) of MTS reagent. Cells were incubated at 37^{o}C for up to 1hr before the absorbance of each well was measured at 490nm. Data were plotted on graphs, with cell viability at each dose of SM being calculated as a % relative to untreated cells (untreated cells designated as 100% viability). Isopropanol alone (0.2% v/v) was not cytotxic. The significance of the observed changes in cell viability were investigated using a paired t-test. Levels of significance were defined as follows: $p < 0.05$ (*), $p < 0.01$ (**) and $p < 0.001$ (***).

2.3. Western blotting

After the indicated treatments, cells were washed in cold phosphate buffered saline (PBS) before lysis in 1X LDS sample buffer (Invitrogen) containing 5% (v/v) 2-mercaptoethanol. Lysates were boiled for 5min prior to sonication to shear the cellular DNA. Protein concentrations were determined using Coomassie Bradford Reagent (Pierce Biotechnology) and 20μg of protein separated on 4-12% bis-tris gels (Invitrogen) using MOPS buffer (Invitrogen) at a constant voltage of 180V for 1h. Proteins were transferred to Hybond-C nitrocellulose membrane (GE Healthcare) using an iBlot machine set at 20V for 13min (Invitrogen). Gel electrophoresis and transfer were performed at room temperature. Membranes were probed using standard protocols, with the following primary antibodies: anti-CHK1 phospho-Ser296 (2349), anti-CHK1 phospho-Ser317 (12302), anti-CHK1 (2360) anti-PARP-1 (9542), anti-cleaved caspase-3 (9664), anti-caspase-9 (9502), anti-H2AX phospho-Ser139 (2577), anti-histone H3 phospho-Ser10 (9701), anti-cdc2(CDK1) phosphor-Tyr15 (9111) and GAPDH (2118), all from Cell Signalling Technologies. Membranes were then washed in TBST (50mM tris pH 7.6, 150mM NaCl and 0.2% Tween20) followed by incubation with the relevant HRP-conjugated secondary antibody. Membranes were washed thoroughly with TBST and visualised using enhanced chemiluminescence (ECL Plus, GE Biosciences). Images were captured using a Syngene G:Box gel documentation system and bands quantified using ImageJ software (http://imagej.nih.gov/ij/). Data were collected from three independent experiments. For quantification of CHK1 phosphorylation, band intensities were normalised to levels of total CHK1 protein. For quantification of all other bands, levels were normalised to the levels of GAPDH.

3. Results

3.1. Activation of CHK1 in cells treated with SM

CHK1 is activated by multi-site phosphorylation mediated by ATM/ATR, resulting in functionally important autophosphorylation at Ser296. To investigate whether CHK1 was activated by SM, a range of human cell lines were exposed to SM for 5h prior to analysis of CHK1 phosphorylation. Multiple human cells were studied to exclude the possibility of cell line-specific effects. In addition, previous studies had demonstrated robust activation of DNA damage signalling events in these cell lines after treatment with 25μM SM for 5h. At this dose and time point there was no evidence of cytotoxicity. The sites analysed were Ser317 and Ser296 (autophosphorylation site). As shown in Figure 1, both sites were robustly and markedly phosphorylated after exposure to SM. For subsequent studies investigating the regulation and functional significance of CHK1 activation, we used two cell lines which demonstrated robust CHK1 phosphorylation and had wild type p53 status and intact p53 responses (HCT 116 and A549). In addition, A549 cells are derived from lung tissue and thus have relevance in terms of sites of SM exposure.

3.2 ATR activates CHK1 after exposure to SM

To investigate whether ATR was involved in the activation of CHK1, a specific kinase inhibitor (AZ 20) was used. Studies showed that 4μM AZ 20 was able to block UV-induced activation of ATR and this concentration was therefore used in this study (data not shown). HCT 116 and A549 cells were pre-treated with AZ 20 before exposure of cells to 25μM SM for 5h and analsyis of CHK1 activation using Western blotting. As shown in Figure 2A and 2B, AZ 20 virtually abolished the SM-induced phosphorylation of CHK1 at both Ser296 and Ser317 in both HCT 116 and A549 cells. These data suggest that ATR is required for CHK1 activation after exposure to SM and that ATR-mediated phosphorylation of Ser317 is necessary before CHK1 can autophosphorylate on Ser296.

3.3. PF 477736 blocks CHK1 activation after exposure to SM

To investigate the functional significance of CHK1 activation after exposure to SM, a specific inhibitor of CHK1 was used (PF 477736). To establish the most appropriate dose of PF 477736 to use in these studies, CHK1 phosphorylation was investigated after UV exposure (widely known to activate CHK1) in cells treated with 20-250nM PF 477736. As shown in Figure 3A, UV caused a marked increase in CHK1 phosphorylation at both Ser296

and 317. Treatment with PF47736 inhibited Ser296 phosphorylation at all doses used but had little or no effect on the ATR target site Ser317. Based on the results in Figure 3A, 100nM PF 477736 was selected as the most appropriate dose to completely block CHK1 activity. To demonstrate that this dose of PF 477736 was able to block SM-induced CHK1 activation, cells were pre-treated with 100nM PF 477736 prior to treatment with SM for 5h and analysis of CHK1 activation using Western blotting. As shown in Figure 3B and 3C, SM caused a marked increase in both Ser296 and Ser317 phosphorylation of CHK1. Consistent with the data after UV treatment, 100nM PF 477736 completely blocked CHK1 activity, assessed by autophosphorylation on Ser296, but did not inhibit ATR-mediated phosphorylation on Ser317. Together, these data show that the kinase activity of CHK1 can be completely blocked by 100nM PF 477736

3.4. Inhibition of CHK1 increases SM cytotoxicity

To investigate the functional significance of CHK1 activation after exposure to SM, the cytotoxicity of SM was measured in cells +/- 100nM PF 477736. This concentration of PF 477736 has previously been shown to completely inhibit CHK1 activation after exposure to SM (see Fig. 3B and 3C). Several human cell lines were pre-treated with 100nM PF 477736 before treatment with SM and measurement of cell viability using an MTS assay. Microscopic inspection of cells revealed high levels of SM-induced cytotoxicity in HEK 293 cells after 24h. Therefore, MTS assays were performed in these cells at this time point. All other cells were left for 48h prior to MTS assay. As shown in Figure 4A, CHK1 inhibition (PF 477736) caused a decrease in cell viability at both 10μM SM and 25μM SM in all cell lines tested, compared to cells with active CHK1 (DMSO). All changes were shown to be statistically significant with the exception of A549 at 10μM SM (+/- PF 477736). To corroborate these findings and to investigate the mechanism of cytotoxicity, the levels of CHK1 phosphorylation and several markers of apoptosis, DNA damage and mitosis were measured in Hela cells using Western blotting. As shown in Figure 4B, SM caused clear phosphorylation of CHK1 on Ser296 at both 10μM and 25μM. Pre-treatment of cells with 100nM PF 477736 completely blocked CHK1 autophosphorylation on Ser296, thus confirming that CHK1 activity was efficiently inhibited in these cells. For markers of apoptosis, the cleavage of PARP-1, caspase-3 and caspase-9 were measured. For DNA damage, the level of H2AX Ser139 phosphorylation was measured. This is a well-validated marker for DNA damage, in particular DNA double strand breaks. Our previous studies

demonstrated H2AX Ser139 phosphorylation (and the formation of H2AX p-Ser139 nuclear foci) after SM, hence the use of H2AX Ser139 as a marker of DNA damage in the current study (Jowsey et al., 2010). For quantification of mitosis, levels of histone H3 Ser10 phosphorylation were measured. To further investigate the progression of cells from G2 phase into mitosis, the phosphorylation of cyclin dependent kinase 1 (CDK1) on Tyr15 was measured. CDK1 activation is required for progression into mitosis and is associated with CDC25C-mediated dephosphorylation of CDK1 Tyr15. As shown in Figure 4B and 4C, all markers of apoptosis were increased in CHK1-inhibited cells after exposure to SM compared to cells with active CHK1, with a concomitant increase in the levels of DNA damage. In addition, SM treatment caused a marked increase in CDK1 Tyr15 phosphorylation (i.e. CDK1 inactivation) and decreased histone H3 Ser10 phosphorylation. These findings are consistent with activation of the G2/M phase checkpoint and the prevention of cells with DNA damage entering mitosis. On the contrary, CHK1 inhibition prevented the SM-induced increase in CDK1 Tyr15 phosphorylation (meaning increased CDK1 activity and defective G2/M phase checkpoint), resulting in increased levels of histone H3 phosphorylation after treatment with SM. Preliminary studies also demonstrated decreased phosphorylation of CDC25C in cells treated with SM+PF 477736 compared to SM alone (data not shown). CDC25C is phosphorylated by CHK1 after DNA damage, causing cytoplasmic retention of CDC25C and decreased dephosphorylation of CDK Tyr15 and thus decreased activation of CDK1.

Together, these data show that inhibition of CHK1 increases the cytotoxicity of SM, with concomitant increases in the levels of apoptosis and DNA damage, along with uncontrolled progression into mitosis.

Discussion

Sulphur mustard is a highly toxic chemical agent that poses a current threat to both civilian and military personnel in the event of a deliberate malicious release. The precise mechanisms mediating the acute and chronic long-term health effects associated with exposure to SM are not fully understood and there is currently no therapeutic option for exposed individuals. It is therefore essential to have a detailed understanding of the molecular effects that SM has upon a cell as well as the cellular mechanisms involved in repairing any damage caused. This study focused on the cell cycle/DNA damage signalling kinase CHK1. The data demonstrated robust activation of this enzyme after exposure to SM in multiple human cell lines. This activation was found to be mediated by the ATR protein kinase. Specific inhibition of CHK1 increased SM cytotoxicity, concomitant with increased markers of apoptosis (cleaved PARP-1/caspase-3/caspase-9), DNA damage (H2AX Ser139) and mitosis (phosphorylated histone H3). Together, these data suggest that CHK1 promotes cell survival after exposure to SM, likely via the regulation of DNA repair processes and blocking entry of damaged cells into mitosis.

DNA damage signalling is initiated by the ATM and ATR kinases, which phosphorylate and activate the checkpoint kinases CHK1 and CHK2 (Smith et al., 2010). Our previous studies have demonstrated the activation of ATM after exposure to SM, monitored by measuring phosphorylation of Ser1981, as well as ATR-dependent phosphorylation of CHK1 at Ser317 (Jowsey et al., 2012). Inhibition of ATM slightly increased SM cytotoxicity, whilst a marked increase in SM toxicity was observed when both ATM and ATR were inhibited. This highlights the importance of DNA damage signalling pathways after exposure to SM. ATM and ATR play important roles, likely due to the variety of DNA lesions induced by SM, including different DNA adducts and crosslinks, which will impede DNA replication and activate ATR. In addition, stalled replication forks and processing of DNA crosslinks, result in the generation and DNA DSBs and subsequent activation of ATM. Other studies have shown the activation of ATM and ATR after exposure of cells to the monofunctional SM analogue 2-chloroethyl ethyl sulphide (CEES) (Jowsey et al., 2009; Tewari-Singh et al., 2010). Whilst phosphorylation of CHK1 at Ser317 and Ser345 has been demonstrated after exposure to SM/CEES, no studies have directly monitored CHK1 autophosphorylation and thus kinase activation. The activation of CHK1 requires multi-site phosphorylation, including Ser317 and Ser345, with mutation of these sites markedly reducing CHK1 kinase activity (Capasso et al., 2002; Walker et al., 2009). Subsequent to Ser317/345 phosphorylation, CHK1 undergoes intramolecular

autophosphorylation on Ser296 (Clarke and Clarke, 2005). Whilst this modification is not essential for the activation of CHK1, it does allow the kinase activity of CHK1 to be conveniently monitored using phospho-specific antibodies. Consistent with the mechanism of CHK1 activation described above, the present study showed that the inhibition of ATR blocked both CHK1 Ser317 phosphorylation and Ser296 autophosphorylation after exposure to SM. In addition, specific inhibition of CHK1 did not decrease phosphorylation of Ser317 but totally blocked autophosphorylation on Ser296 after exposure to SM.

Whilst phosphorylation of CHK1 at Ser296 is not essential for the activation of CHK1, it does have important functional significance. Expression of a CHK1 Ser296Ala mutant in CHK1-deficient cells results in inefficient G2/M arrest after UV and uncontrolled progression into mitosis (Kasahara et al., 2010). This is consistent with our observation that inhibition of CHK1, and thus loss of Ser296 phosphorylation, resulted in markedly increased histone H3 phosphorylation (a marker of mitosis) after exposure to SM. This finding was further supported by decreased CDC25C Ser216 phosphorylation (data not shown) and decreased CDK1 Tyr15 phosphorylation in cells treated with SM+PF 477736 compared to SM alone. These data strongly suggests that PF 477736 prevents CHK1-mediated phosphorylation of CDC25C. CDC25C thus remains in the nucleus and dephosphorylates CDK1 Tyr15, resulting in CDK1 activation and unwanted progression of cells into mitosis. Our data also demonstrated that CHK1 inhibition increased SM toxicity in multiple human cell lines, concomitant with increased levels of multiple apoptosis markers. This could be a result of the uncontrolled progression of DNA damaged cells into mitosis and subsequent 'mitotic catastrophe'. Other studies have demonstrated that inhibition of CHK1 sensitises cells to crosslinking agents such as carboplatin and cisplatin, with proposed mechanisms involving inefficient G2/M phase arrest (Blasina et al., 2008; Thompson et al., 2012).

The present study also demonstrated increased levels of histone H2AX Ser139 phosphorylation in CHK1-inhibited cells after exposure to SM. Phosphorylation of this protein has been demonstrated after multiple genotoxic agents and generally correlates with levels of cellular DNA damage. Our previous studies have demonstrated clear phosphorylation of H2AX Ser139 after exposure to SM as well as the formation of H2AX nuclear foci, representing sites of DNA DSBs (Jowsey et al., 2010). The levels of Ser139 phosphorylation and number of nuclear foci were markedly increased in cells lacking homologous recombination repair (HRR). CHK1 contributes to HRR by phosphorylation of RAD51 and promoting the formation of RAD51 filaments on single-stranded DNA, prior to strand invasion/exchange with an undamaged sister chromatid (Bahassi et al., 2008; Sorensen

et al., 2005). Whilst further studies will be required to verify this, it is likely that CHK1 inhibition reduces the efficiency of HRR after exposure to SM, resulting in increased levels of DSBs, increased H2AX Ser139 phosphorylation and increased cell death. In addition, CHK1 contributes to the s-phase checkpoint as well as the stabilisation of stalled replication forks (e.g. at sites of DNA crosslinks) (Smith et al., 2010). Defects in both of these processes (in cells treated with SM+PF 477736) would also result in increased levels of DNA DSBs and increased H2AX Ser139 phosphorylation. Our data also demonstrated that the effect of CHK1 inhibition on SM toxicity was most significant in Hela cells, with an approximate 2-fold increase in SM toxicity observed, compared to cells with active CHK1. Interestingly, these cells lack p53 responses due to Human Papilloma Virus-mediated down-regulation of p53, rendering the cells effectively p53 null. As a result, Hela cells have a defective p53-mediated G1/S phase arrest, thus allowing SM-damaged cells to progress into S/G2/M phases of the cell cycle. Whilst the lack of G1/S phase arrest alone is likely to increase SM toxicity, this effect will be further exacerbated by inhibition of CHK1 and the previously described effects on the G2/M checkpoint. There has been considerable interest in the use of CHK1 inhibitors in combination therapy for cancer. For example, given that the majority of tumours have mutant p53 and thus lack efficient G1/S-phase arrest, it was hypothesised that inhibition of CHK1 (and thus abrogation of S-phase and G2/M checkpoints) would potentiate the effects of chemotherapy agents. A recent study demonstrated that this was not the case, with siRNA-mediated knockdown of CHK1 and treatment with irinotecan (a topoisomerase I inhibitor) or cisplatin showing similar toxicity in p53-proficient and –deficient cells (Zenvirt et al., 2010). This is in contrast to the present study, where CHK1 inhibition increased SM toxicity in all cell lines tested, though by far the greatest effect was observed in Hela cells, which do not express p53. This suggests that cells lacking functional p53 are more sensitive to the combined toxic effect of CHK1 inhibition and SM, than cells expressing wild-type p53. We are currently investigating whether thus effect is specific to SM or whether is also observed in response to clinically relevant compounds related to SM, such as nitrogen mustards. These studies will also be performed in isogenic cell line pairs (+/- p53).

In order to better understand the toxic mechanism of SM and develop potential therapeutic procedures, it is necessary to have a detailed understanding of the cellular biochemical changes associated with exposure to this agent. The present study demonstrated robust activation of CHK1 in multiple human cell lines after exposure to SM. Specific inhibition of CHK1 rendered cells more sensitive to SM toxicity with increased levels of

apoptosis, likely due to defects in homologous recombination repair and premature entry of SM-exposed cells into mitosis.

Acknowledgements

This Research was supported by the National Institute for Health Research Health Protection Research Unit in Chemical and Radiation Threats and Hazards at Newcastle University. The views expressed are those of the author(s) and not necessarily those of the NIHR or the Department of Health.

References

Abraham, R.T., 2004. Pi 3-Kinase Related Kinases: 'Big' Players in Stress-Induced Signaling Pathways. DNA Repair (Amst) 3, 883-887.

Ashby, J., Tinwell, H., Callander, R.D., Clare, N., 1991. Genetic Activity of the Human Carcinogen Sulphur Mustard Towards Salmonella and the Mouse Bone Marrow. Mutat Res 257, 307-311.

Bahassi, E.M., Ovesen, J.L., Riesenberg, A.L., Bernstein, W.Z., Hasty, P.E., Stambrook, P.J., 2008. The Checkpoint Kinases Chk1 and Chk2 Regulate the Functional Associations between Hbrca2 and Rad51 in Response to DNA Damage. Oncogene 27, 3977-3985.

Balali-Mood, M., Hefazi, M., 2005. The Pharmacology, Toxicology, and Medical Treatment of Sulphur Mustard Poisoning. Fundam Clin Pharmacol 19, 297-315.

Balali-Mood, M., Hefazi, M., 2006. Comparison of Early and Late Toxic Effects of Sulfur Mustard in Iranian Veterans. Basic Clin Pharmacol Toxicol 99, 273-282.

Balali-Mood, M., Hefazi, M., Mahmoudi, M., Jalali, E., Attaran, D., Maleki, M., Razavi, M.E., Zare, G., Tabatabaee, A., Jaafari, M.R., 2005. Long-Term Complications of Sulphur Mustard Poisoning in Severely Intoxicated Iranian Veterans. Fundam Clin Pharmacol 19, 713-721.

Blasina, A., Hallin, J., Chen, E., Arango, M.E., Kraynov, E., Register, J., Grant, S., Ninkovic, S., Chen, P., Nichols, T., O'Connor, P., Anderes, K., 2008. Breaching the DNA Damage Checkpoint Via Pf-00477736, a Novel Small-Molecule Inhibitor of Checkpoint Kinase 1. Mol Cancer Ther 7, 2394-2404.

Capasso, H., Palermo, C., Wan, S., Rao, H., John, U.P., O'Connell, M.J., Walworth, N.C., 2002. Phosphorylation Activates Chk1 and Is Required for Checkpoint-Mediated Cell Cycle Arrest. J Cell Sci 115, 4555-4564.

Clarke, C.A., Clarke, P.R., 2005. DNA-Dependent Phosphorylation of Chk1 and Claspin in a Human Cell-Free System. Biochem J 388, 705-712.

Fidder, A., Moes, G.W., Scheffer, A.G., van der Schans, G.P., Baan, R.A., de Jong, L.P., Benschop, H.P., 1994. Synthesis, Characterization, and Quantitation of the Major Adducts Formed between Sulfur Mustard and DNA of Calf Thymus and Human Blood. Chem Res Toxicol 7, 199-204.

Foote, K.M., Blades, K., Cronin, A., Fillery, S., Guichard, S.S., Hassall, L., Hickson, I., Jacq, X., Jewsbury, P.J., McGuire, T.M., Nissink, J.W., Odedra, R., Page, K., Perkins, P., Suleman, A., Tam, K., Thommes, P., Broadhurst, R., Wood, C., 2013. Discovery of 4-{4-[(3r)-3-Methylmorpholin-4-Yl]-6-[1-(Methylsulfonyl)Cyclopropyl]Pyrimidin-2-Y L}-1h-Indole (Az20): A Potent and Selective Inhibitor of Atr Protein Kinase with Monotherapy in Vivo Antitumor Activity. J Med Chem 56, 2125-2138.

Ghabili, K., Agutter, P.S., Ghanei, M., Ansarin, K., Panahi, Y., Shoja, M.M., 2011. Sulfur Mustard Toxicity: History, Chemistry, Pharmacokinetics, and Pharmacodynamics. Crit Rev Toxicol 41, 384-403.
Hurley, P.J., Bunz, F., 2007. Atm and Atr: Components of an Integrated Circuit. Cell Cycle 6, 414-417.
Jowsey, P.A., Williams, F.M., Blain, P.G., 2009. DNA Damage, Signalling and Repair after Exposure of Cells to the Sulphur Mustard Analogue 2-Chloroethyl Ethyl Sulphide. Toxicology 257, 105-112.
Jowsey, P.A., Williams, F.M., Blain, P.G., 2010. The Role of Homologous Recombination in the Cellular Response to Sulphur Mustard. Toxicol Lett 197, 12-18.
Jowsey, P.A., Williams, F.M., Blain, P.G., 2012. DNA Damage Responses in Cells Exposed to Sulphur Mustard. Toxicol Lett 209, 1-10.
Kasahara, K., Goto, H., Enomoto, M., Tomono, Y., Kiyono, T., Inagaki, M., 2010. 14-3-3gamma Mediates Cdc25a Proteolysis to Block Premature Mitotic Entry after DNA Damage. EMBO J 29, 2802-2812.
Mahmoudi, M., Hefazi, M., Rastin, M., Balali-Mood, M., 2005. Long-Term Hematological and Immunological Complications of Sulfur Mustard Poisoning in Iranian Veterans. Int Immunopharmacol 5, 1479-1485.
Patil, M., Pabla, N., Dong, Z., 2013. Checkpoint Kinase 1 in DNA Damage Response and Cell Cycle Regulation. Cell Mol Life Sci 70, 4009-4021.
Saladi, R.N., Smith, E., Persaud, A.N., 2006. Mustard: A Potential Agent of Chemical Warfare and Terrorism. Clin Exp Dermatol 31, 1-5.
Smith, J., Tho, L.M., Xu, N., Gillespie, D.A., 2010. The Atm-Chk2 and Atr-Chk1 Pathways in DNA Damage Signaling and Cancer. Adv Cancer Res 108, 73-112.
Sorensen, C.S., Hansen, L.T., Dziegielewski, J., Syljuasen, R.G., Lundin, C., Bartek, J., Helleday, T., 2005. The Cell-Cycle Checkpoint Kinase Chk1 Is Required for Mammalian Homologous Recombination Repair. Nat Cell Biol 7, 195-201.
Tewari-Singh, N., Gu, M., Agarwal, C., White, C.W., Agarwal, R., 2010. Biological and Molecular Mechanisms of Sulfur Mustard Analogue-Induced Toxicity in Jb6 and Hacat Cells: Possible Role of Ataxia Telangiectasia-Mutated/Ataxia Telangiectasia-Rad3-Related Cell Cycle Checkpoint Pathway. Chem Res Toxicol 23, 1034-1044.
Thompson, R., Meuth, M., Woll, P., Zhu, Y., Danson, S., 2012. Treatment with the Chk1 Inhibitor Go6976 Enhances Cisplatin Cytotoxicity in Sclc Cells. Int J Oncol 40, 194-202.
Walker, M., Black, E.J., Oehler, V., Gillespie, D.A., Scott, M.T., 2009. Chk1 C-Terminal Regulatory Phosphorylation Mediates Checkpoint Activation by De-Repression of Chk1 Catalytic Activity. Oncogene 28, 2314-2323.
Zenvirt, S., Kravchenko-Balasha, N., Levitzki, A., 2010. Status of P53 in Human Cancer Cells Does Not Predict Efficacy of Chk1 Kinase Inhibitors Combined with Chemotherapeutic Agents. Oncogene 29, 6149-6159.
Zhang, Y., Hunter, T., 2014. Roles of Chk1 in Cell Biology and Cancer Therapy. Int J Cancer 134, 1013-1023.
Zhao, H., Piwnica-Worms, H., 2001. Atr-Mediated Checkpoint Pathways Regulate Phosphorylation and Activation of Human Chk1. Mol Cell Biol 21, 4129-4139.

Figure Legends

Fig. 1. Activation of CHK1 in cells treated with SM. (A) HCT 116, SH-SY5Y, Hela, A549 and HEK 293 cells were treated with 25μM SM for 5h prior to investigation of CHK1 activation using Western blotting with the indicated antibodies. (B) Quantification of the Western blot data in (A) using ImageJ software. Data is presented as level of Ser296 or Ser317 normalised to total CHK1 and represents the mean and standard deviation of three independent experiments.

Fig. 2. ATR-dependent activation of CHK1 after exposure to SM. (A) HCT 116 and A549 cells were treated with 4μM AZ 20 (or DMSO control) for 45min prior to treatment with 25μM SM for 5h. The activation of CHK1 was then investigated using Western blotting with the indicated antibodies. (B) Quantification of the Western blot data in (A) using ImageJ software. Data is presented as level of Ser296 or Ser317 normalised to total CHK1 and represents the mean and standard deviation of three independent experiments.

Fig. 3. PF 477736 blocks CHK1 activation after exposure to UV and SM. (A) HCT 116 and A549 cells were treated with 20-250nM PF 477736 for 45min prior to treatment with UV for 1h. The activation of CHK1 was then investigated using Western blotting with the indicated antibodies. (B) HCT 116 and A549 cells were treated with 100nM PF 477736 for 45min prior to treatment with 25μM SM for 5h. The activation of CHK1 was then investigated using Western blotting with the indicated antibodies. (C) Quantification of the Western blot data in (B) using ImageJ software. Data is presented as level of Ser296 or Ser317 normalised to total CHK1 and represents the mean and standard deviation of three independent experiments.

Fig. 4. Inhibition of CHK1 enhances SM toxicity. (A) HCT 116, A549, Hela and HEK 293 cells were treated with 100nM PF 477736 for 45 min prior to treatment with isopropanol ('untreated control'), 10μM SM or 25μM SM. Cell viability was then measured using an MTS assay after 24h for HEK 293 cells and 48h for all other cells. Data is presented as % viability relative to untreated cells and represents the mean and standard deviation from three independent experiments. The significance of the observed changes in cell viability between DMSO- and PF 477736-treated cells were investigated using a paired t-test. Levels of significance were defined as follows: $p < 0.05$ (*), $p < 0.01$ (**) and $p < 0.001$ (***). NS =

not significant. (B) Hela cells treated as in (A) were analysed by Western blotting with the indicated antibodies. (C) Quantification of the Western blot data in (B) using ImageJ software. Levels of Ser296 and Ser317 were normalised to total CHK1 levels. The levels of all other proteins/phosphorylation sites were normalised to GAPDH. Data represents the mean and standard deviation from three independent experiments.

Figure 1

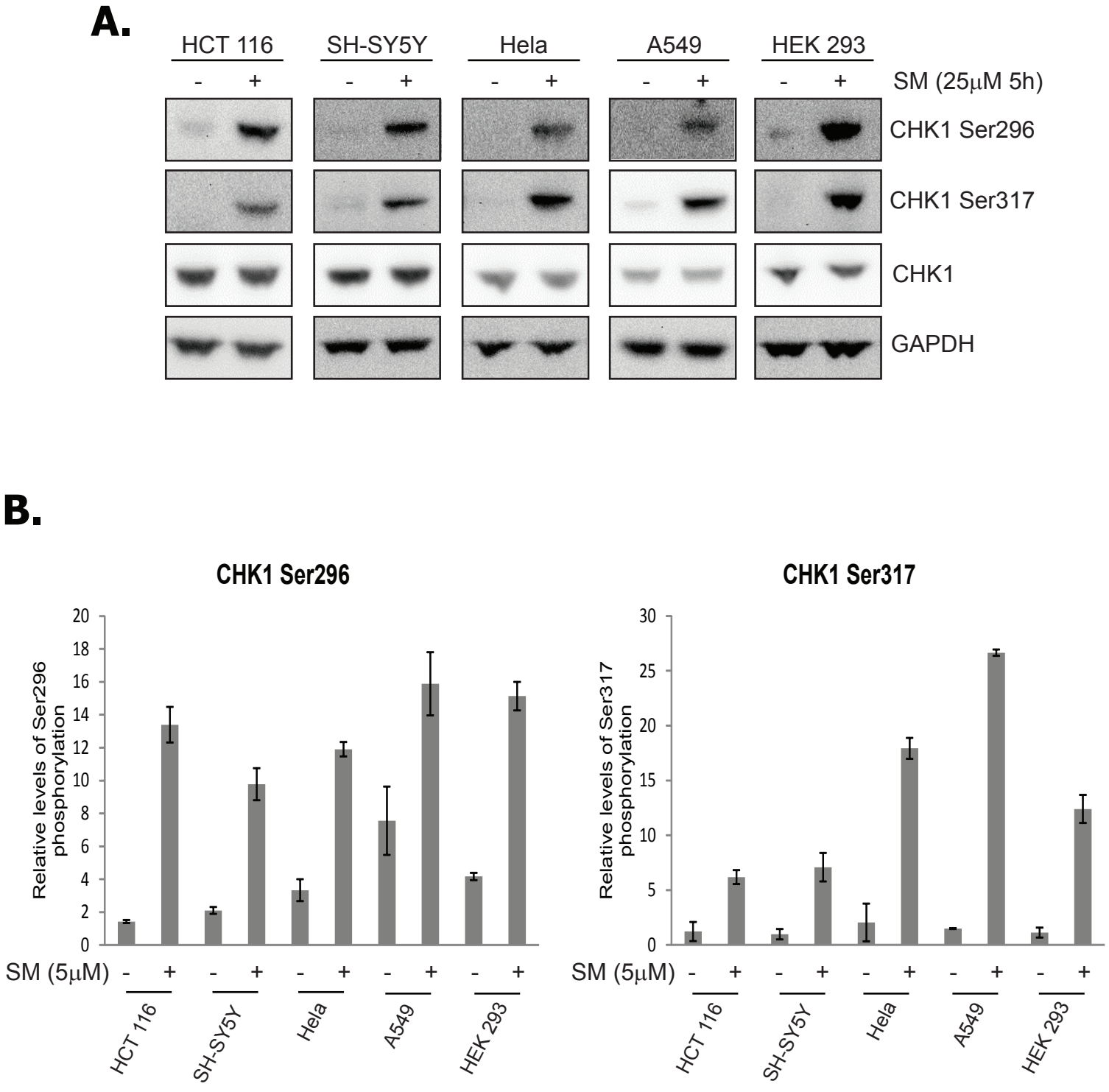

Jowsey et al., 2014

Figure 2

A.

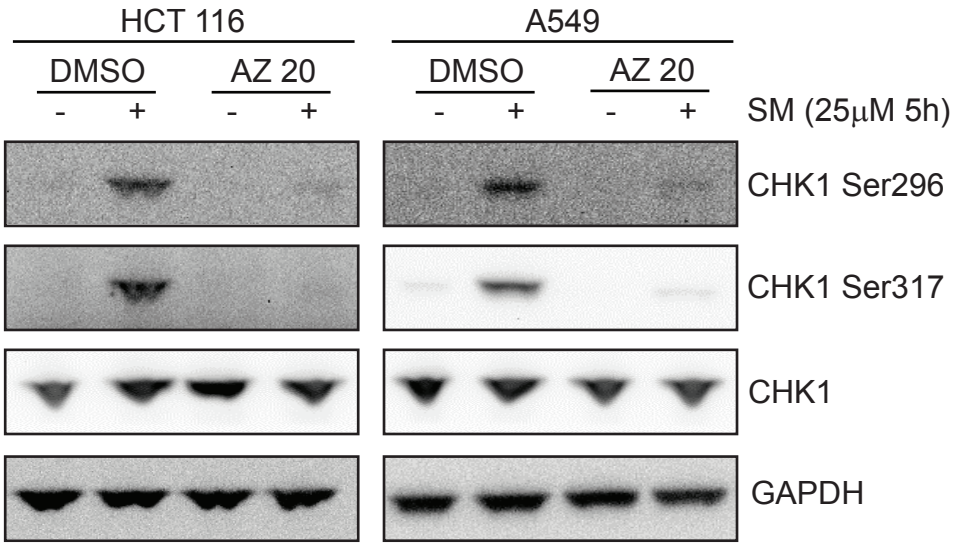

B.

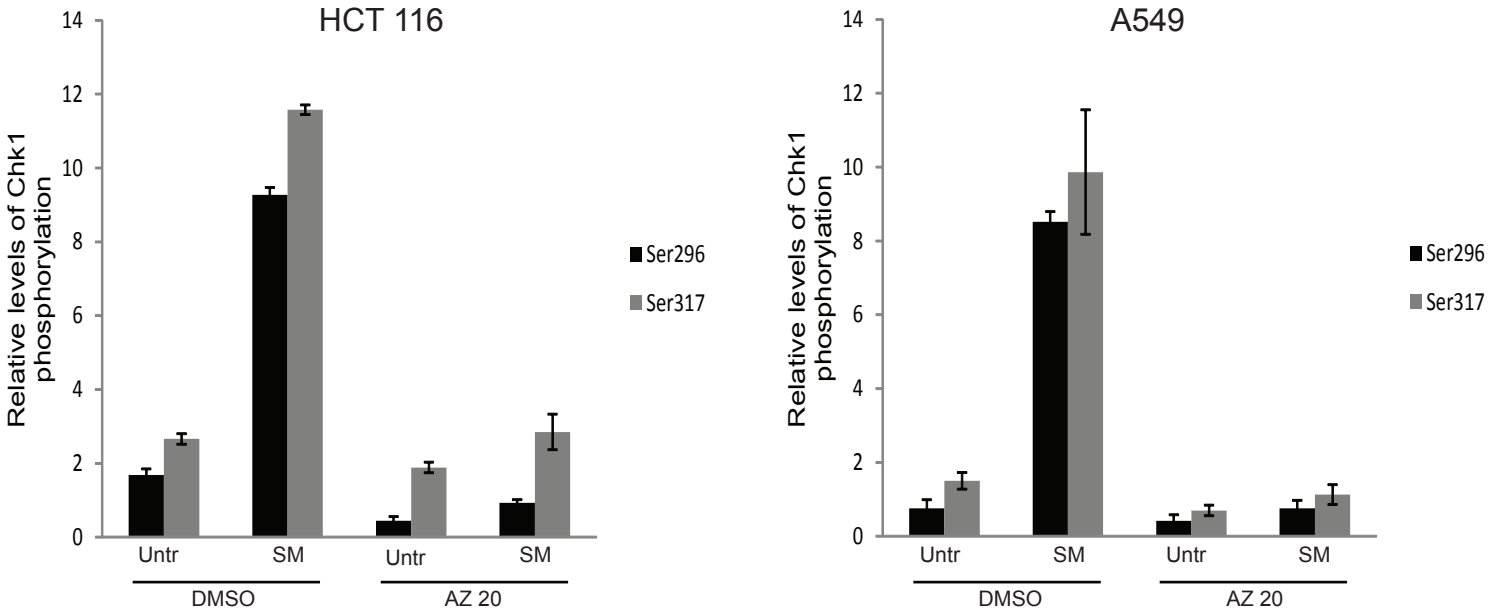

Jowsey et al., 2014

Figure 3

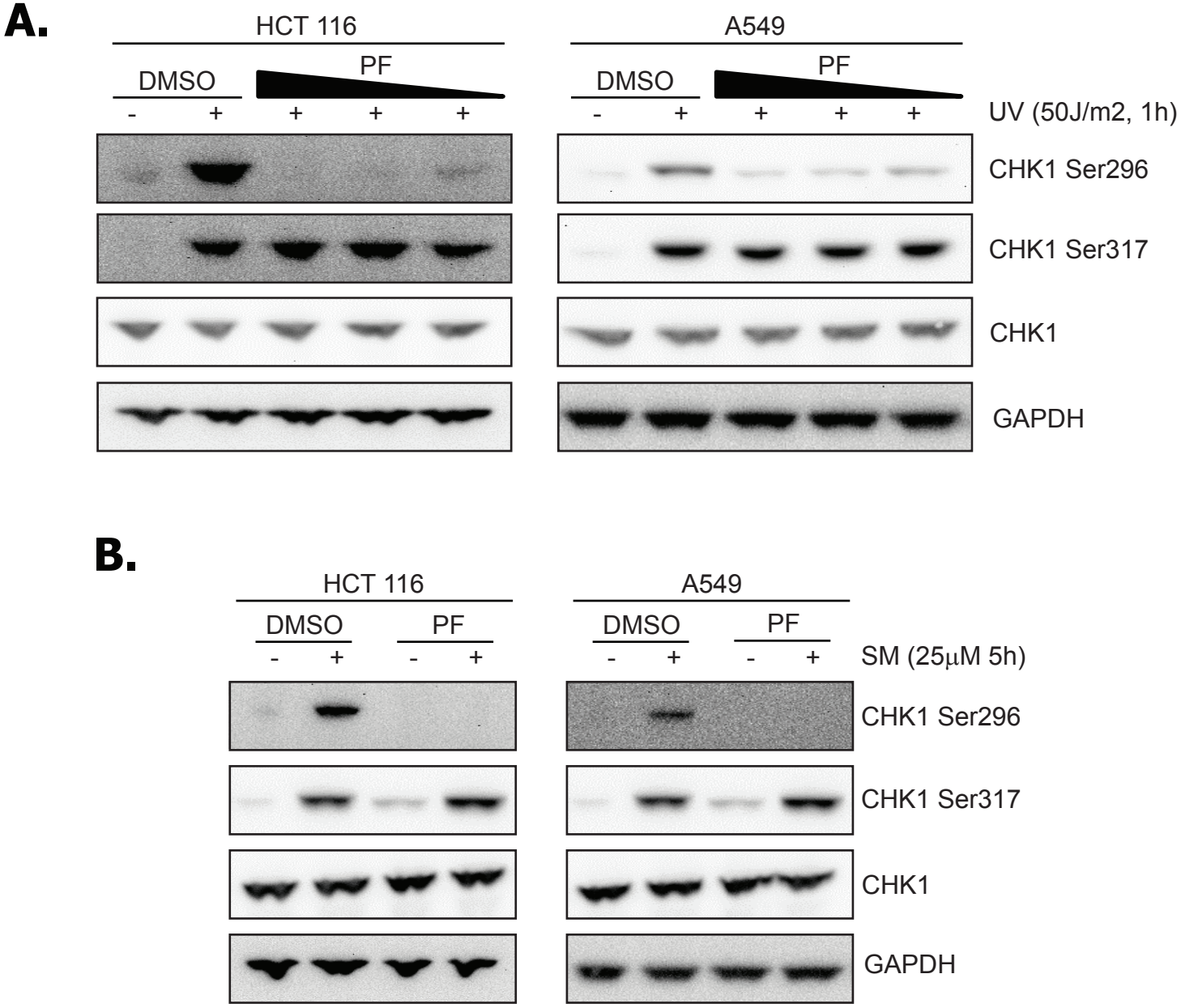

Jowsey et al., 2014

Figure 4

A.

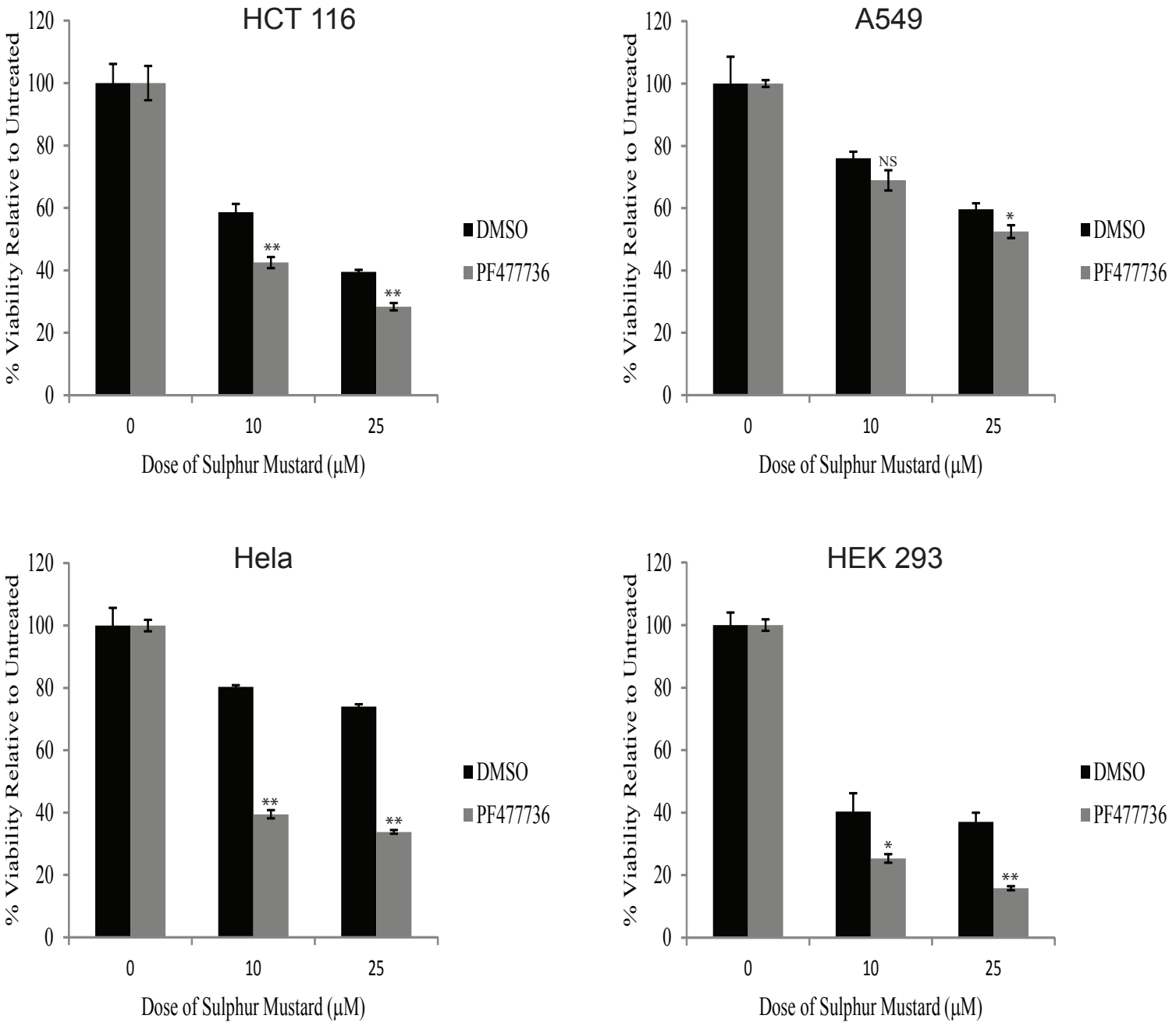

Jowsey et al., 2014

Figure 4

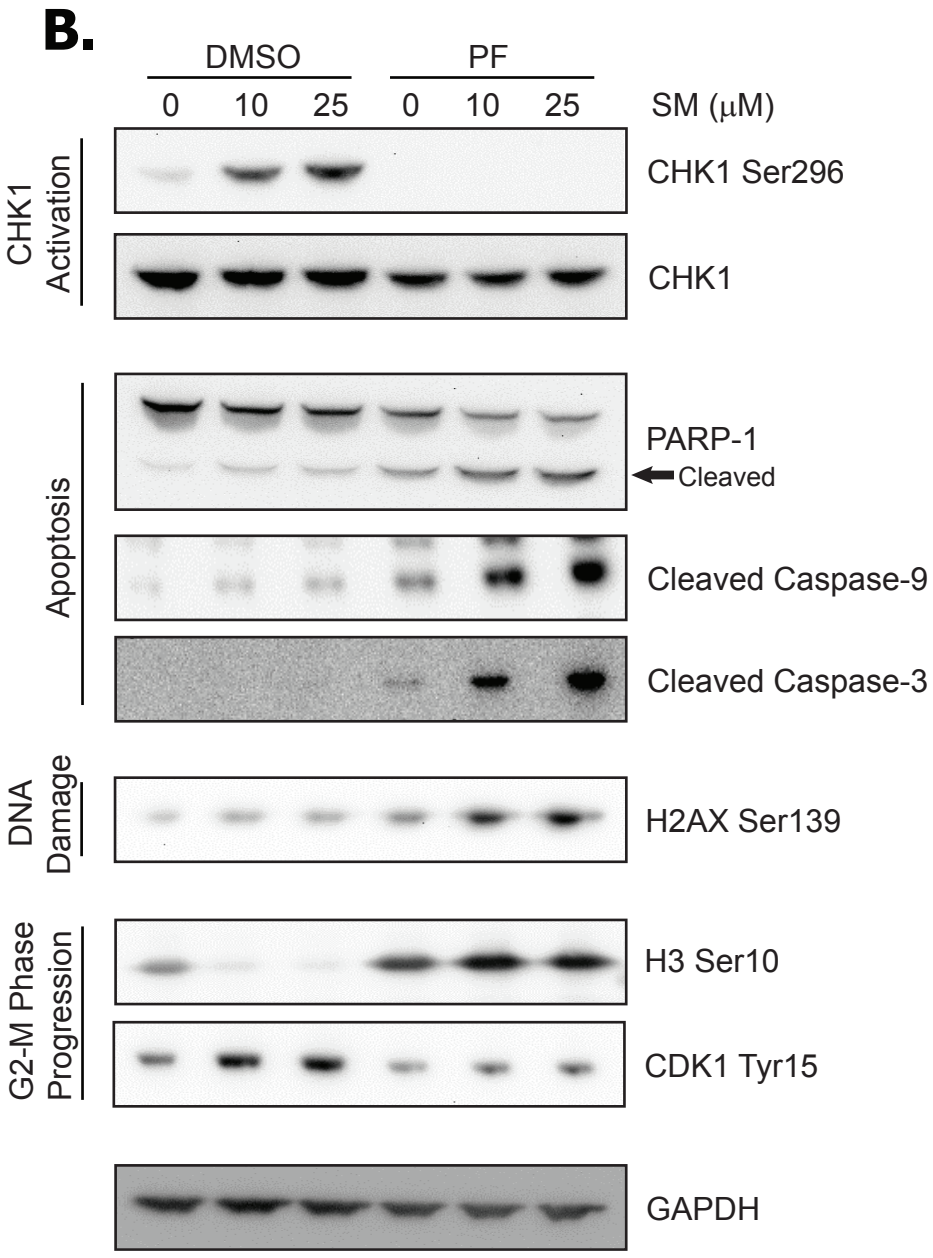

Jowsey et al., 2014

Figure 4

C.

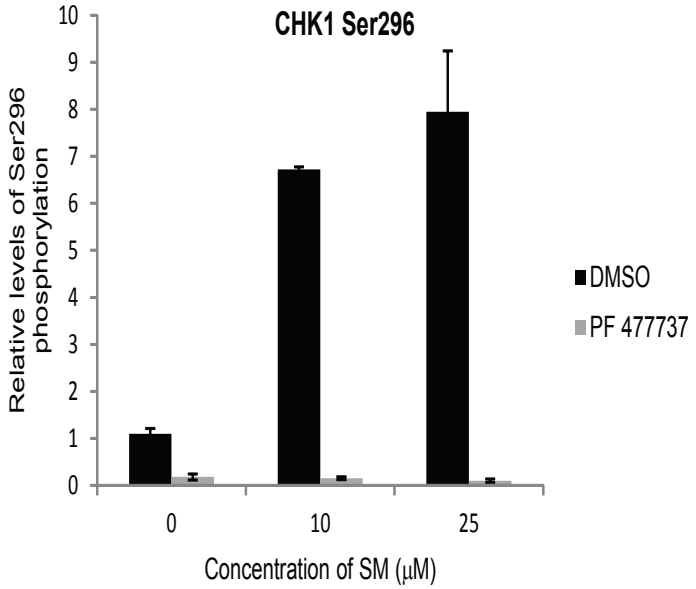

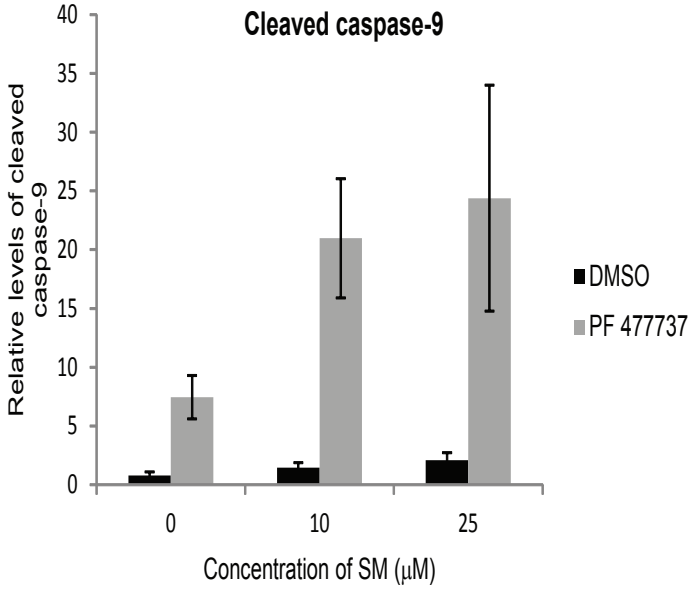

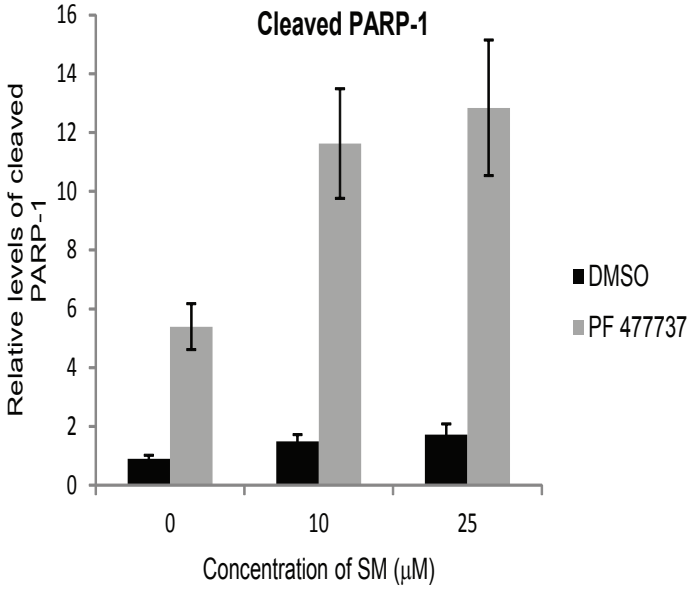

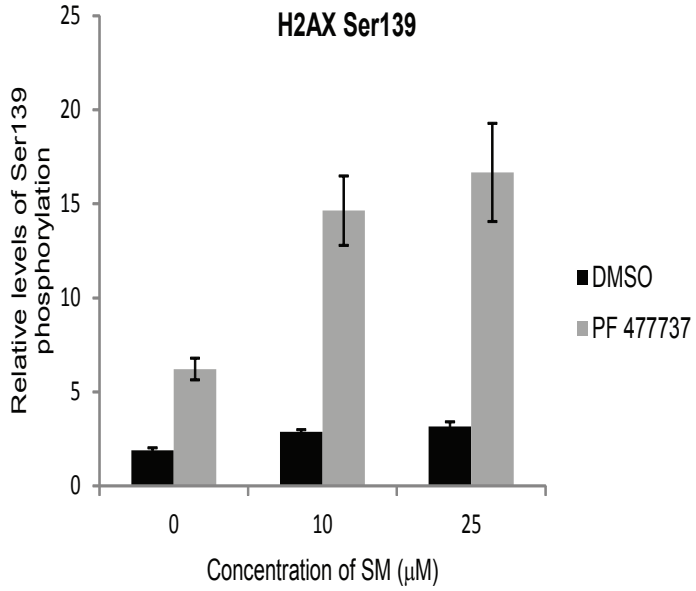

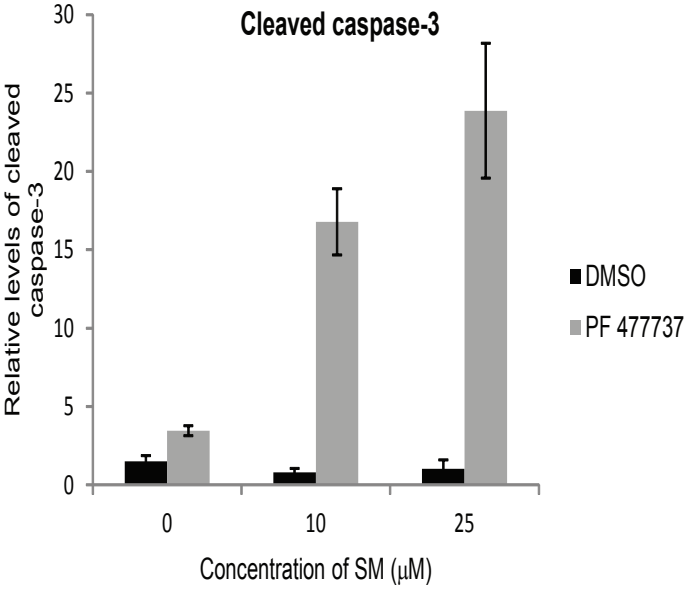

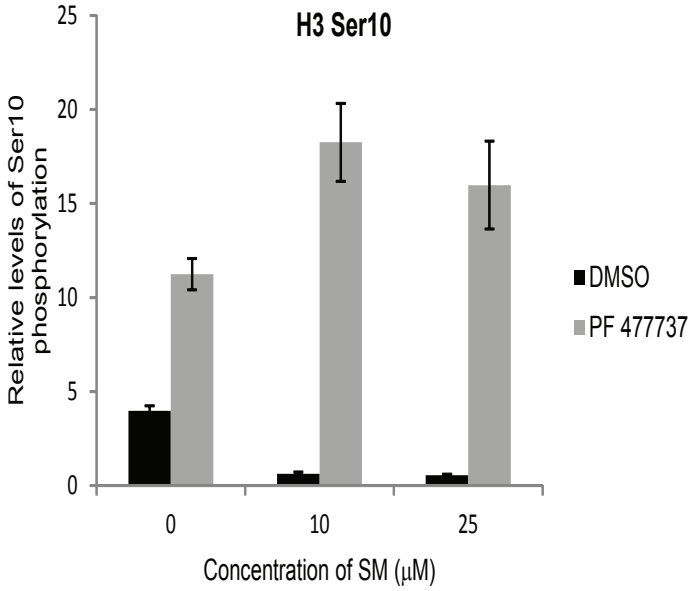

Jowsey et al., 2014

Figure 4

C.

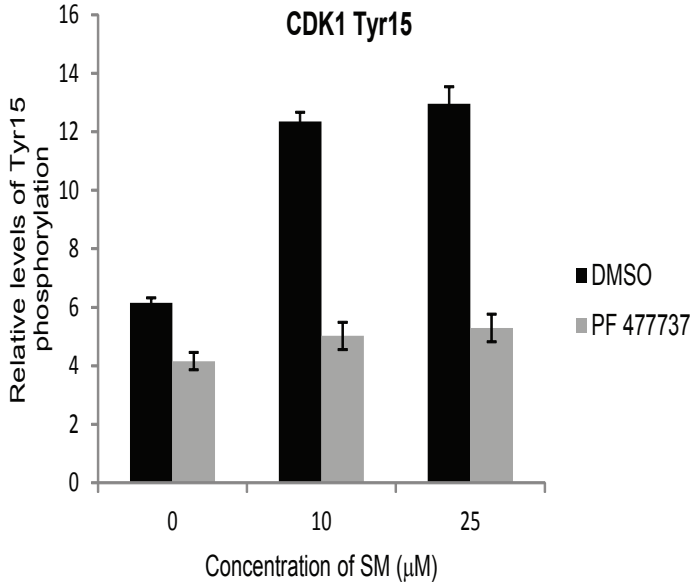

Jowsey et al., 2014